



Convenient two-dimensional model for design of fuel channels for proton exchange membrane fuel cells

Falin Chen^{a,*}, Ying-Zhi Wen^a, Hsin-Sen Chu^b, Wei-Mon Yan^c, Chyi-Yeou Soong^d

^a Institute of Applied Mechanics, National Taiwan University, Taipei 106, Taiwan, ROC

^b Department of Mechanical Engineering, National Chiao Tung University, Hsin-Chu 300, Taiwan, ROC

^c Department of Mechatronic Engineering, Huaan University, Shih-Ting, Taipei 22305, Taiwan, ROC

^d Department of Aeronautical Engineering, Feng Chia University, Seatwen, Taichung 40745, Taiwan, ROC

Received 6 August 2003; accepted 10 October 2003

Abstract

A theoretical, two-dimensional, along-the-channel model has been developed to design fuel channels for proton exchange membrane (PEM) fuel cells. This has been implemented by solving the resultant ordinary differential equation with a straightforward shooting computational scheme. With such a design tool, an analysis can be made of the effects due to some operation and design parameters, such as inlet velocity, inlet pressure, catalyst activity, height of channel, and porosity of gas-diffusion layer to obtain a fuel cell with high performance. Present results indicate that there is always a trade-off between higher power density and higher efficiency of the fuel cell. Namely, a design for higher power density (a better performance) is always accompanied with a higher fuel efficiency (or a larger fuel consumption rate and a higher fuel cost), and vice versa. When some relevant physical parameters are determined experimentally and applied in the present model, a quantitative design for a fuel cell of high efficiency or performance is feasible.

© 2003 Published by Elsevier B.V.

Keywords: Fuel channels; Proton exchange membrane fuel cells; Gas-diffusion layer

1. Introduction

The proton exchange membrane (PEM) fuel cell is an electrochemical device which combines fuel (hydrogen) and oxidant (oxygen) to produce electricity, and water and heat are the major by-products. In past decades, substantial efforts [1–4] have been devoted to reducing the cost as well as promoting the efficiency of the fuel cell. In this respect, the design of high-efficiency fuel channels is one of the important issues [5–19]. Several different types of fuel channels have been used in practical designs, such as straight channels, serpentine channels, and interdigitate channels. The morphology of the channel also varies, namely, meander, spiral or straight types. For a meander or a spiral channel, the length may be several meters long. In such a long channel, the fuel may be entirely consumed before exit, which implies that a certain portion of the cell may not have fuel for chemical reactions. That is, a part of the cell may not produce any electrons during operation and this reduces the efficiency. Therefore, analysis of the channel flow becomes

a necessity in fuel cell design and an efficient and convenient theoretical model for channel analysis is essential.

To date, there have been two major approaches for the analysis of channel flow. One uses computational fluid dynamic (CFD) techniques to examine the two- or three-dimensional flow in fuel channels [5–10], the other uses a one-dimensional approximation approach to investigate the variation of flow structure and includes the fuel concentration as well as the current generated along the channel [11–19]. In the CFD approaches, mathematical models are usually developed for the whole PEM fuel cell, which may consider the conservation of mass, momentum and energy, equations governing the electrochemical reaction, and various kinds of physical properties of the components such as diffusivity of the gas-diffusion layer, electro-osmosis in membrane, fuel convection across the membrane, chemical reaction and activity in catalyst layers, and membrane hydration [20–23]. With this approach, however, the computation is rather time-consuming and the analysis procedure is so tedious that the computation of the whole flow field in channels becomes inefficient and is sometimes even an unnecessary step to obtain the fuel cell design.

* Corresponding author. Tel.: +886-2-363-0979; fax: +886-2-363-9290.
E-mail address: falin@spring.iam.ntu.edu.tw (F. Chen).

Nomenclature

\tilde{c}	dimensionless concentration
C	concentration (mol m^{-3})
C_0	inlet concentration (mol m^{-3})
F	Faraday constant ($96,500 \text{ C mol}^{-1}$)
h	channel height (m)
i	local current density (A m^{-2})
i_0	inlet current density (A m^{-2})
K_i	$i = 1-5$, constants in Eq. (15)
L	channel length (m)
M	molar weight (kg mol^{-3})
n	transferred electron number
P	pressure (Pa)
P_0	inlet pressure (atm)
\bar{P}	pressure gradient (Pa m^{-1})
R	universal gas constant ($8.314 \text{ J mol}^{-1} \text{ K}^{-1}$)
T	gas temperature (K)
u	velocity in x -direction (m s^{-1})
u_0	inlet velocity in x -direction (m s^{-1})
\bar{u}	cross-sectional averaged velocity in x -direction
\tilde{u}	dimensionless velocity in x -direction
v	velocity in y -direction (m s^{-1})
V_0	suction velocity (m s^{-1})

Greek letters

α	charge transfer coefficient
γ	reaction order
η	over potential (V)
μ	viscosity ($\text{kg m}^{-1} \text{ s}^{-1}$)
ξ	empirical constant regarding the slip condition at the porous boundary
ρ	density (kg m^{-3})

two-phase flows. In these studies, however, the channel flow was assumed to have a constant velocity along the channel. Under most circumstances, however, this assumption may result in significant discrepancies with reality.

In the present work, a two-dimensional theoretical model is developed and the includes a continuity equation, momentum equations and the Tafel equation. At the bottom of the channel, the consumption of fuel due to chemical reactions is modeled by way of sucking the fuel through the porous boundary. This model allows investigation of the variations of the flow structure, the fuel concentration, and the current density along the channel. A systematic parametric study is implemented to examine the influence of relevant design and operation parameters on the effective length of the fuel channel. Specifically, the effects due to the inlet velocity and pressure and the porosity of the gas-diffusion layer at the bottom can be investigated. The activity of the catalyst attached to the gas diffusion layer can also be analyzed.

2. The theoretical model

Two-dimensional horizontal channel flow shown schematically in Fig. 1. The channel has a constant height and is sufficiently long that the conditions at both the entrance and the exit do not affect the flow of the domain under consideration. The fluid, either hydrogen in the anode or oxygen in the cathode, is assumed to be an ideal gas. Since the flow velocity is so high, the variation of temperature along the channel is assumed to be negligible. It is also assumed that the bipolar plate in which the fuel channel is built is an ideal collecting electrode with no ohmic loss. The overpotential can then be maintained at a constant value along the channel [12]. As a result, the local current density is a function of the fuel concentration at each specific position [7]. For such a chemically active flow, the continuity equation is:

$$\frac{\partial \rho}{\partial t} + \frac{\partial(\rho u)}{\partial x} + \frac{\partial(\rho v)}{\partial y} = 0, \tag{1}$$

in which $u = u(x, y)$ and $v = v(x, y)$ are the velocity in the x - and y -directions, respectively. Due to the fact that the channel height is very small compared with the channel length, it may be assumed that the density distribution across

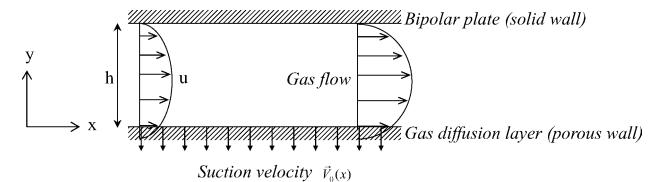


Fig. 1. Schematic description of flow considered. Two-dimensional viscous flow is bounded between bipolar plate (solid wall) at top and gas-diffusion layer (porous wall) at bottom. Velocity profile is essentially a parabolic curve. Because of the porous wall there is a velocity slip at bottom. Because of chemical reaction in the gas-diffusion layer, there is a suction flow across the porous wall, accounted for by suction velocity $\bar{V}_0(x)$.

A more efficient and convenient scheme, which can to some extent reach the goal of fuel cell design both quantitatively and qualitatively, is the channel model [11–19]. Since the flow passes the fuel channel very rapidly, cross-sectional variations of flow structure and other physical parameters such as fuel concentration, fuel density and fuel temperature can be ignored. A major concern is the variation of the relevant physical properties along the channel. It was found that the along-the-channel model is much simplified and that the equations can be solved more conveniently and efficiently. Recently, several along-the-channel models have been developed for the above-mentioned purpose. Nguyen and co-workers [10,11] have proposed a set of governing equations which include water and energy transport across the membrane and have considered heat removal along the channel. Other workers [12–14] have examined the gas dynamics, concentration decay and current drop along the channel. Argyropoulos et al. [15–19] have investigated the pressure drop and the temperature variation along the channel by considering the mass and energy conservation of

122 the channel is uniform, i.e., $\rho = \rho(x)$. Because $\rho(x) =$
 123 $MC(x)$, Eq. (1) can be converted to:

$$124 \frac{\partial(Cu)}{\partial x} + \frac{\partial(Cv)}{\partial y} = 0. \quad (2)$$

125 Integrating Eq. (2) along y and applying Leibnitz's rule
 126 gives:

$$127 C \frac{\partial}{\partial x} \int_0^h u \, dy + \frac{dC}{dx} \int_0^h u \, dy + C \int_0^h \frac{\partial v}{\partial y} \, dy = 0. \quad (3)$$

128 By letting $\bar{u}(x) \equiv (1/h) \int_0^h u(x, y) \, dy$ be the averaged veloc-
 129 ity over the cross-section of the channel and by applying
 130 the non-slip condition at the top $u(x, h) = 0$ and the slip
 131 condition at the bottom $u(x, 0) = \xi \bar{u}(x)$, we obtain:

$$132 h \frac{d[C(x)\bar{u}(x)]}{dx} = C(x)v(x, 0) = -C(x)V_0(x), \quad (4)$$

133 where V_0 is the suction velocity along the bottom of channel,
 134 which is defined as $V_0 = (1/nF)(i(x)/C(x))$. Thus, Eq. (4)
 135 becomes:

$$136 \frac{d[C(x)\bar{u}(x)]}{dx} = -\frac{1}{h} \frac{i(x)}{nF}. \quad (5)$$

137 The relation between the overpotential η and the electric
 138 current density i is governed by the Tafel equation:

$$139 i(x) = i_0 \left[\frac{C(x)}{C_0} \right]^\gamma \exp \left(\frac{\alpha F}{RT} \eta \right), \quad (6)$$

140 so that the suction velocity V_0 can be expressed by:

$$141 V_0(x) = \left[\frac{1}{nF} \frac{i_0}{C_0^\gamma} \exp \left(\frac{\alpha F}{RT} \eta \right) \right] C^{\gamma-1}(x). \quad (7)$$

142 Note that, the slip boundary condition at the bot-
 143 tom $u(x, 0) = \xi \bar{u}(x)$ is derived from the so-called
 144 Beavers–Joseph boundary condition at the interface be-
 145 tween a fluid and a porous layer [24], and the parameter
 146 ξ essentially accounts for the permeability of the porous
 147 media since the factor due to the velocity gradient at the
 148 bottom is absorbed into the averaged velocity $\bar{u}(x)$. Given
 149 that the velocity gradient does not change significantly
 150 along the channel, a change in ξ may be seen as a change in
 151 the permeability or, equivalently, a change in the porosity
 152 of the porous medium below. In the present study, it con-
 153 sidered that ξ varies from 0.1 to 1 [24] due to the fact that
 154 the porosity of the gas-diffusion layer at the bottom is high.

155 For the momentum equation, it is assumed that, for the
 156 present two-dimensional channel flow, the velocity in the
 157 x -direction is much larger than that in the y -direction. After
 158 applying order analysis on the momentum equations (or the
 159 Navier–Stokes equations) in both x - and y -directions, a single
 160 momentum equation results, as follows:

$$161 \rho(x) \left[u \frac{\partial u}{\partial x} + v \frac{\partial u}{\partial y} \right] = -\frac{dP}{dx} + \mu \frac{\partial^2 u}{\partial y^2}. \quad (8)$$

162 The pressure gradient along the channel is assumed to be
 163 constant, i.e., $(dP/dx) = \text{constant} = \bar{P}$. Under the normal

operating conditions of a 1 kW fuel cell, $\bar{P} = 12 \text{ Pa m}^{-1}$ 164
 [2,12–14], which is to be used in the present analysis. Inte- 165
 166 grating Eq. (8) along the height yields:

$$MC \int_0^h \left[u \frac{\partial u}{\partial x} + v \frac{\partial u}{\partial y} \right] dy = -h\bar{P} + \mu \frac{\partial u}{\partial y} \Big|_0^h. \quad (9) \quad 167$$

To simplify Eq. (9) further, it is assumed that $u(x, y)$ is a 168
 quasi-parabolic velocity profile [25] defined as $u(x, y) =$ 169
 $A(x)y^2 + B(x)y + G(x)$. At $y = 0$, $u(x, 0) = \xi \bar{u}(x)$ and 170
 this leads to $G(x) = \xi \bar{u}(x)$; at $y = h$, $u(x, y) = 0$ and 171
 $B(x) = -ha(x) - (\xi/h)\bar{u}(x)$. To obtain $A(x)$, the non-slip 172
 boundary condition is applied at the top $u(x, h) = 0$ and 173
 this results in $A(x) = -(6/h^2)(1 - (1/2)\xi)\bar{u}(x)$. As a result, 174
 the approximated velocity function in x -direction is 175
 obtained as: 176

$$177 u(x, y) = \bar{u}(x) \left[-6 \left(1 - \frac{1}{2}\xi \right) \frac{y^2}{h^2} + 2(3 - 2\xi) \frac{y}{h} + \xi \right]. \quad (10) \quad 178$$

This equation implies that the horizontal velocity is a 180
 second-order parabolic function of y , with a small slip at 181
 the bottom of channel, as shown schematically in Fig. 1. 182
 To obtain $v(x, h)$, Eq. (10) is substitute in Eq. (8) and the 183
 resultant equation is integrated along y and the bound- 184
 ary conditions of v are applied at the top and the bottom 185
 of the channel, i.e., $v(x, h) = 0$ and $v(x, 0) = V_0(x)$, 186
 yielding: 188

$$189 v(x, y) = \frac{[C(x)\bar{u}(x)]'}{C(x)} \left[2 \left(1 - \frac{1}{2}\xi \right) \frac{y^2}{h^2} - (3 - 2\xi) \frac{y}{h} - \xi y \right] \quad (11) \quad 190$$

$$- V_0(x).$$

Eqs. (10) and (11) are substituted in Eq. (9) to give the 191
 following equation for the channel flow: 193

$$194 \left(\frac{2}{15}\xi^2 - \frac{1}{5}\xi + \frac{6}{5} \right) \frac{d[C(x)\bar{u}^2(x)]}{dx} + \frac{\xi}{h} C(x)\bar{u}(x)V_0(x) \quad 194$$

$$+ \frac{\bar{P}}{M} + 12 \left(1 - \frac{1}{2}\xi \right) \frac{\mu}{Mh^2} \bar{u}(x) = 0. \quad (12) \quad 195$$

Eqs. (5), (6) and (12) are the governing equations for the 196
 two-dimensional flow along the channel, in which the vari- 197
 ations of the fuel concentration $C(x)$, the velocity $u(x)$ and 198
 the current density $i(x)$ are to be solved. Since these equa- 199
 tions have an initial value problem, the initial velocity at the 200
 entrance, u_0 , and the initial concentration fed to the channel, 201
 C_0 , are required. It is therefore assumed that $\tilde{u}(x) = \bar{u}(x)/u_0$ 202
 and $\tilde{c}(x) = C(x)/C_0$ and two relationships are substituted 203
 these into the equations to give: 204

$$205 \frac{d(\tilde{c}\tilde{u})}{dx} + K_1 \tilde{c}^\gamma = 0, \quad (13)$$

$$206 K_2 \frac{d(\tilde{c}\tilde{u}^2)}{dx} + K_3 + K_4 \tilde{c}^\gamma \tilde{u} + K_5 \tilde{u} = 0, \quad (14)$$

207 where

$$\begin{aligned}
 K_1 &= \frac{i_0}{nFhC_0u_0} \exp\left(\frac{\alpha F}{RT}\eta\right), \\
 K_2 &= \frac{2}{15}\xi^2 - \frac{1}{5}\xi + \frac{6}{5}, \\
 K_3 &= \frac{\bar{P}}{MC_0u_0^2}, \\
 K_4 &= \xi \frac{i_0}{nFhC_0u_0} \exp\left(\frac{\alpha F}{RT}\eta\right), \\
 K_5 &= 12 \left(1 - \frac{1}{2}\xi\right) \frac{\mu}{Mh^2C_0u_0}.
 \end{aligned}
 \tag{15}$$

209 The initial conditions become $\tilde{u} = 1$ and $\tilde{c} = 1$. These two
 210 equations are solved by a fourth order Runge–Kutta scheme.
 211 Eqs. (13) and (14) are the two simplified equations for the
 212 averaged horizontal velocity \tilde{u} and averaged fuel concentra-
 213 tion \tilde{c} . After obtaining these two values, the Tafel equation
 214 (Eq. (6)) can be applied to obtain the local current density
 215 along the channel. The combination of these equations
 216 and the shooting scheme becomes a convenient tool to de-
 217 termine various physical parameters relevant to the design
 218 of fuel channels of PEM fuel cells. This scheme is differ-
 219 ent from those developed in other studies [11–19] in which
 220 the velocity variations in both x - and y -directions were ig-
 221 nored and only the effective length was considered. Using
 222 this simplified model, allows not only examination of the
 223 effective length of the fuel channel under various operation
 224 conditions, but also the effects due to relevant design and
 225 operation parameters on the fuel cell performance.

226 **3. Typical flow field: an example**

227 Analyses in the present and the following sections are
 228 made on the basis of the base case; the values of its relevant
 229 physical parameters are shown in Table 1. This case essen-
 230 tially corresponds to a 1 kW PEM fuel cell under normal
 231 operation conditions [2,12–14]. The results in terms of the
 232 variations of velocity, fuel concentration and current den-
 233 sity along the channel are presented in Fig. 2. It is found
 234 that the fuel concentration decays monotonically along the
 235 channel due to the chemical reaction occurring at the bot-
 236 tom of channel, while the flow velocity increases along the
 237 channel because of the depletion of fuel downstream. Both
 238 effects are the direct consequence of fuel consumption along
 239 the channel, which in turn leads to a decrease in generated
 240 current (Fig. 2(b)) because of, again, the depletion of fuel
 241 downstream. These findings suggest that variations of these
 242 physical properties occur simultaneously, and therefore will
 243 be considered as a whole instead of separately as in previ-
 244 ous studies [11–19] Also the velocity is taken as constant
 245 while the fuel concentration changes along the channel.

246 The generation of current density decreases along the
 247 channel because of the decay in fuel concentration (see
 248 Fig. 2(b)). Note that, for the present base case, the fuel con-

Table 1

Values of physical parameters of base case corresponding to 1 kW PEM fuel cell [2,12–14].

Channel side	Cathode
Gas flow	Oxygen
Half-reaction	$O_{2(g)} + 4H^+ + 4e^- \rightarrow 2H_2O$
Channel temperature, T (K)	353.15
Inlet gas velocity, u_0 ($m\ s^{-1}$)	0.1
Inlet gas pressure, P_0 (atm)	2
Inlet gas concentration, C_0 ($mol\ m^{-3}$)	69.00
Exchange current density, i_0 ($A\ m^{-2}$)	10^{-5}
Activation overpotential, η (V)	0.3
Reaction order, γ	0.5
Electrons transferred in reaction, n	4
Charge-transfer coefficient, α	2.0
Molar weight, M ($kg\ mol^{-1}$)	32×10^{-3}
Viscosity, μ ($kg\ m\ s^{-1}$)	2×10^{-5}
Channel height, h (m)	10^{-3}
Channel length, L (m)	0.1
Pressure gradient, \bar{P} ($Pa\ m^{-1}$)	10
Universal gas constant, R ($J\ mol^{-1}\ K^{-1}$)	8.314
Faraday constant, F ($C\ mol^{-1}$)	96500
Slip velocity fraction, ξ	0.1
K_1 (m^{-1})	13.77
K_2	1.181
K_3 (m^{-1})	452.9
K_4 (m^{-1})	1.377
K_5 (m^{-1})	1032.6

249 centration decrease by about 50% and the local current den-
 250 sity by about 25% within the 10 cm long channel. The vari-
 251 ations in these two parameters are very significant for such
 252 a short distance, and imply that an accurate calculation of
 253 the effective channel length cannot be ignored in the design
 254 of a high-efficiency fuel cell. In a practical sense, too long a
 255 channel will result in a large dead region in the bipolar plate,

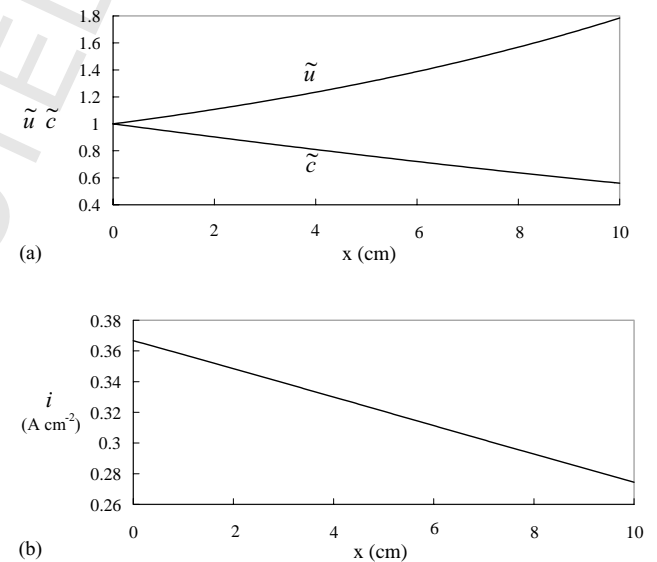


Fig. 2. Along-the-channel variations of major quantities of present problem: (a) dimensionless velocity \tilde{u} and concentration \tilde{c} ; (b) generated current density. Results are calculated on basis of base case shown in Table 1.

256 while too short a channel will cause a great part of the fuel
 257 to leave the cell without reaction. A long channel gives a low
 258 local current density downstream (or a low performance of
 259 the fuel cell) but, with respect of fuel consumption, a long
 260 channel length may ensure that the fuel is consumed before
 261 leaving the exit. The latter will result in better efficiency of
 262 gas usage.

263 4. Physical parameter effects

264 Several physical parameters have significant effects on the
 265 channel flow, which may in turn affect both the design and
 266 operation conditions of the fuel cell. These physical param-

eters include the flow velocity at the inlet, the fuel concen- 267
 tration, the activity of the catalyst, the channel height, and 268
 the porosity of the gas-diffusion layer. The following exam- 269
 ines the physical effects due to these five parameters with 270
 special attention to their influence on the effective length of 271
 the channel. When the effect of a particular physical param- 272
 eter is considered, this parameter will be change systemat- 273
 ically while the other four physical parameters are fixed at 274
 the values shown in Table 1. 275

4.1. Effect of inlet velocity 276

The variation of flow velocity, fuel concentration and local 277
 current density along the channel are shown in Fig. 3(a)–(c),

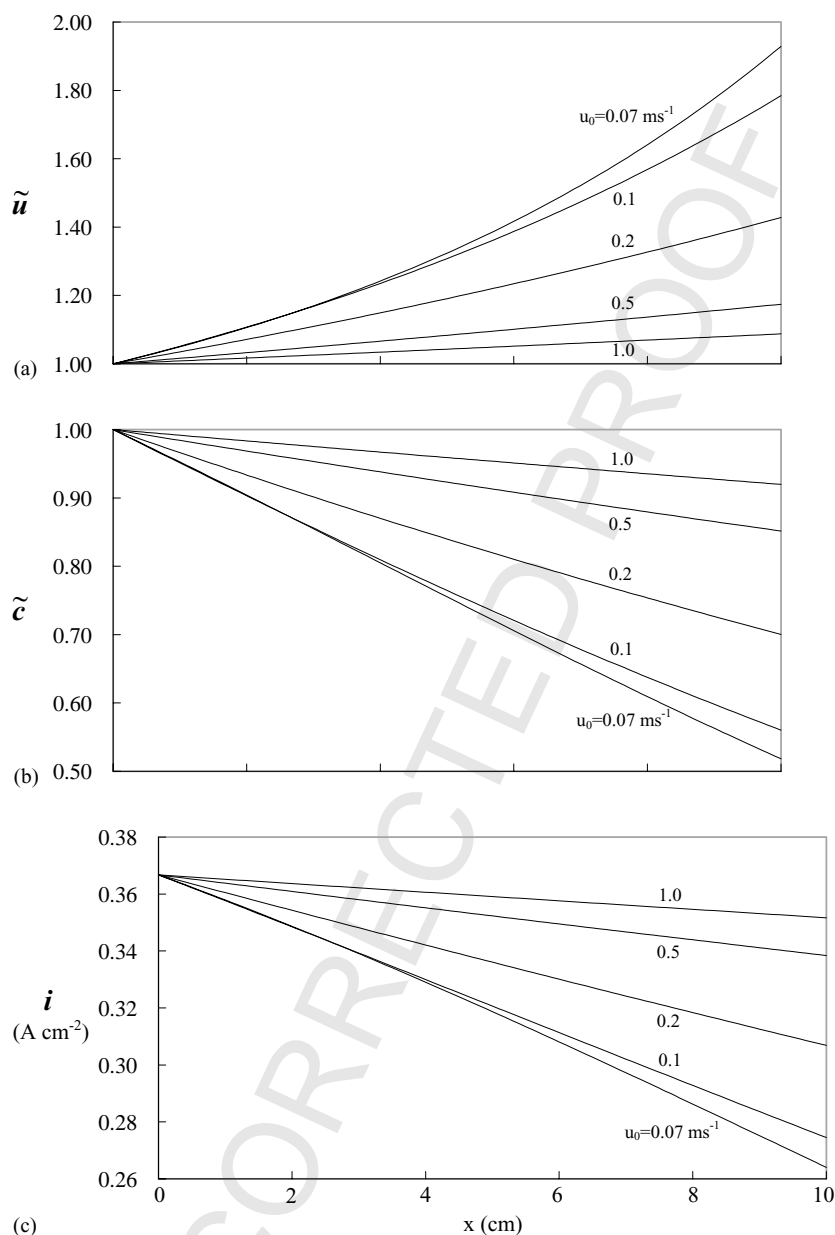


Fig. 3. Effects of inlet velocity on along-the-channel variations of: (a) dimensionless velocity \tilde{u} ; (b) dimensionless concentration \tilde{c} ; (c) local current density.

278 respectively, for variation in inlet velocity from 0.07 to
 279 1 m s^{-1} . For a lower inlet velocity, because the fuel has more
 280 time to diffuse into the active layer at the bottom to react,
 281 the fuel concentration decays more rapidly (Fig. 3(b)). De-
 282 crease in fuel concentration leads to an increase in flow ve-
 283 locity in accordance with the conservation of mass (Fig. 3(a))
 284 and results in a larger decrease in the local current density
 285 due to the higher depletion of fuel or a lower reaction rate
 286 (Fig. 3(c)). It is interesting to note that, for an inlet veloc-
 287 ity of 1 m s^{-1} , the changes in flow velocity, fuel concentra-
 288 tion and local current density along the channel are all very
 289 small. As a result, practically, if a uniformly high current

density along the channel (and thus a higher power density) 290
 is required, then a larger inlet fuel velocity can be applied 291
 to the cell, but at the expense of a higher fuel consumption 292
 rate. On the other hand, if the fuel efficiency is the major 293
 concern, it is necessary to apply a lower inlet velocity so 294
 that the fuel consumption (and thus the reaction) along the 295
 channel can be implemented more completely. 296

4.2. Effect of fuel concentration 297

From the equation of state of an ideal gas, i.e., $C_0 =$ 298
 P_0/RT , the fuel concentration is a function of the partial

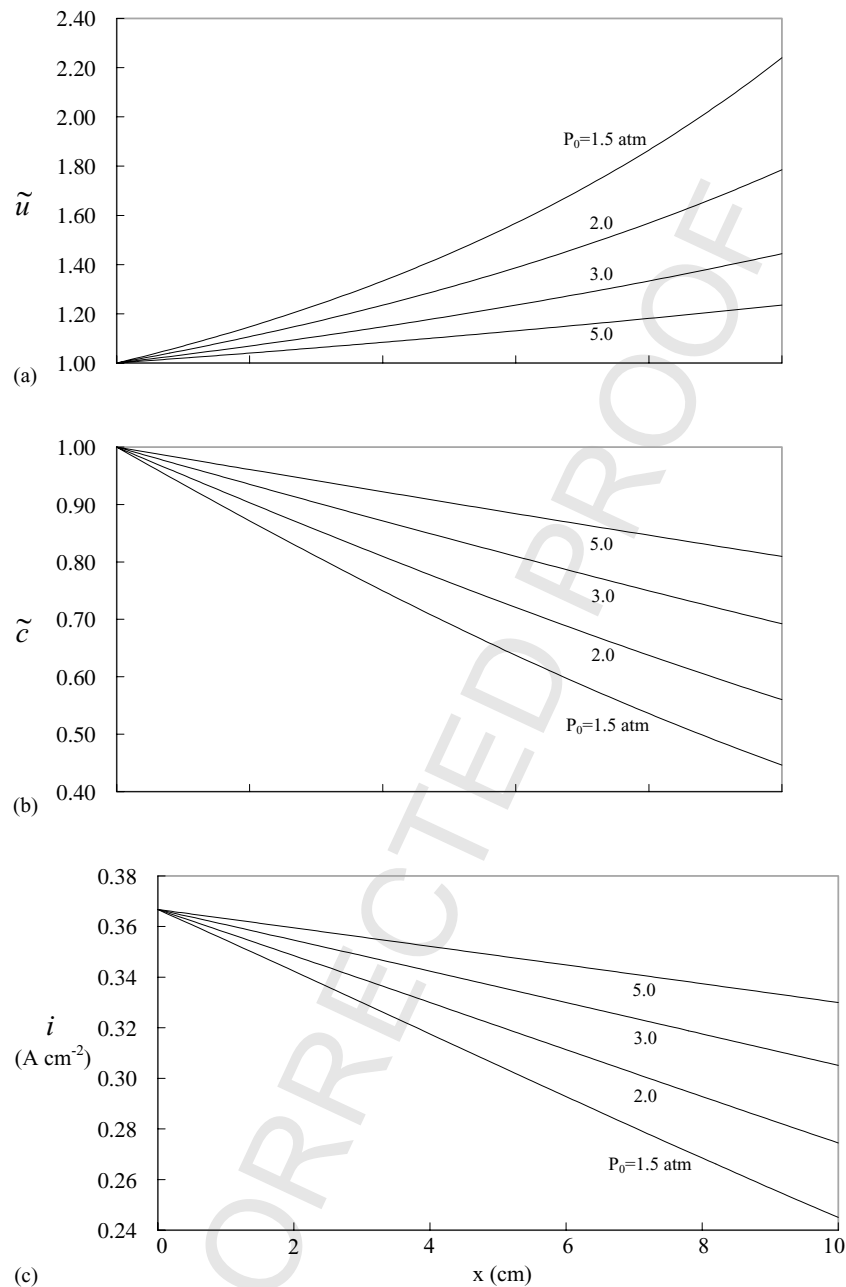


Fig. 4. Effects of inlet fuel pressure on along-the-channel variations of: (a) dimensionless velocity \tilde{u} ; (b) dimensionless concentration \tilde{c} ; (c) local current density.

299 pressure of the fuel gas. Accordingly, the change in fuel con-
 300 centration can be attributed to the change in partial pressure
 301 of the fuel. Thus, to examine the effects of fuel concentra-
 302 tion, the inlet pressure P_0 of the fuel was changed from 1.5
 303 to 5 atm. The results are presented in Fig. 4(a)–(c) and show
 304 that for a higher inlet pressure (or a higher fuel concentra-
 305 tion), and thus a larger pressure gradient along the channel
 306 when the pressure at outlet is assumed to be constant, the
 307 increase in flow velocity along the channel is smaller (but
 308 the overall velocity is higher) (Fig. 4(a)) because the con-
 309 sumption rate of the fuel along the channel is smaller (and
 310 the decrease of the fuel concentration along the channel is
 311 smaller) (see Fig. 4(b)). Due to the smaller fuel consumption

rate, the decrease in current density along the channel is also
 312 smaller. As a result, to ensure that the current density along
 313 the channel can be uniformly high, or equivalently to have a
 314 fuel cell of higher power density, the cell must be supplied
 315 with a fuel of higher concentration (a higher inlet pressure)
 316 but, again, at the expense of a higher fuel consumption rate.
 317

4.3. Effect of catalyst activity

The activity of the catalyst can be indicated by the value of
 319 the overpotential η , which can be converted into the current
 320 density i by the Tafel equation (Eq. (6)). The present analy-
 321 sis considers three different activities, corresponding to three

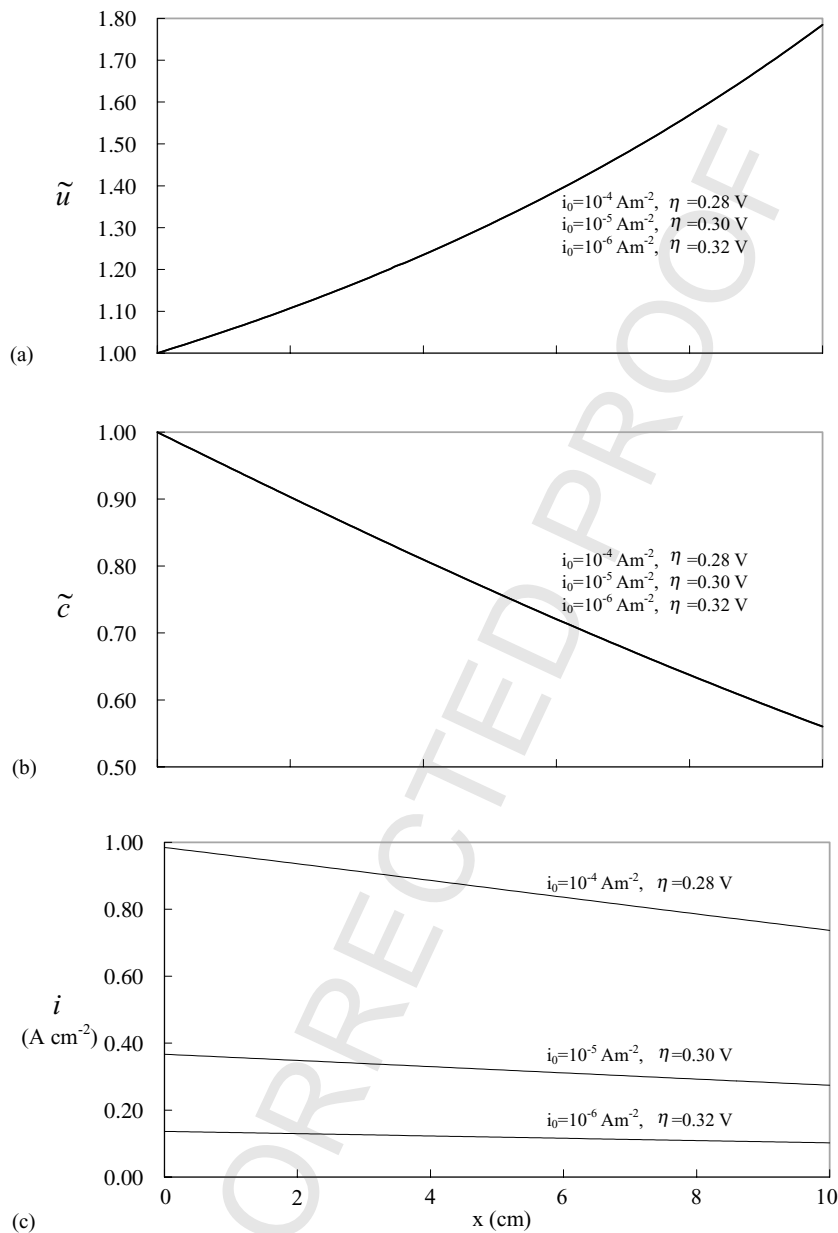


Fig. 5. Effects imposed by different catalysts on along-the-channel variations of: (a) dimensionless velocity \tilde{u} ; (b) dimensionless concentration \tilde{c} ; (c) local current density.

322 overpotentials $\eta = 0.28, 0.30$ and 0.32 V. The corresponding
 323 current densities are $i_0 = 10^{-4}, 10^{-5}$ and 10^{-6} A cm $^{-2}$. A
 324 catalyst of higher activity leads to a faster reaction rate and
 325 thus a faster speed of electron generation and, accordingly
 326 corresponds to a lower overpotential loss and a higher cur-
 327 rent density. Note that, a different catalyst activity implies
 328 a different fuel consumption rate, which can be reflected by
 329 the change in suction velocity V_0 at the bottom of the chan-
 330 nel (see Eq. (7)).

331 The results shown in Fig. 5(a)–(c) illustrate that the differ-
 332 ence in activity of the catalyst examined in the present study
 333 does not result in an obvious difference in either the flow
 334 velocity (Fig. 5(a)) or the fuel concentration (Fig. 5(b)), be-
 335 cause the curves of different activities virtually overlap each
 336 other. On the other hand, it has a significant effect on the lo-

337 cal current density, as shown in Fig. 5(c), namely: a higher
 338 catalyst activity leads to a higher local current density and
 339 results in a slightly more rapid decrease along the channel.
 340 This indicates that an efficient scheme to raise the fuel cell
 341 performance without consuming more fuel is to use a cata-
 342 lyst of higher activity. This is a common scenario accepted
 343 by fuel cell researchers, world-wide. Accordingly, the de-
 344 velopment of a high-activity catalyst for PEM fuel cells has
 345 been a major research issue, or may be the most important
 346 one.

4.4. Effect of channel height

347
 348 Since it is assumed that the fuel is well mixed across the
 channel height, a larger height of channel is equivalent to

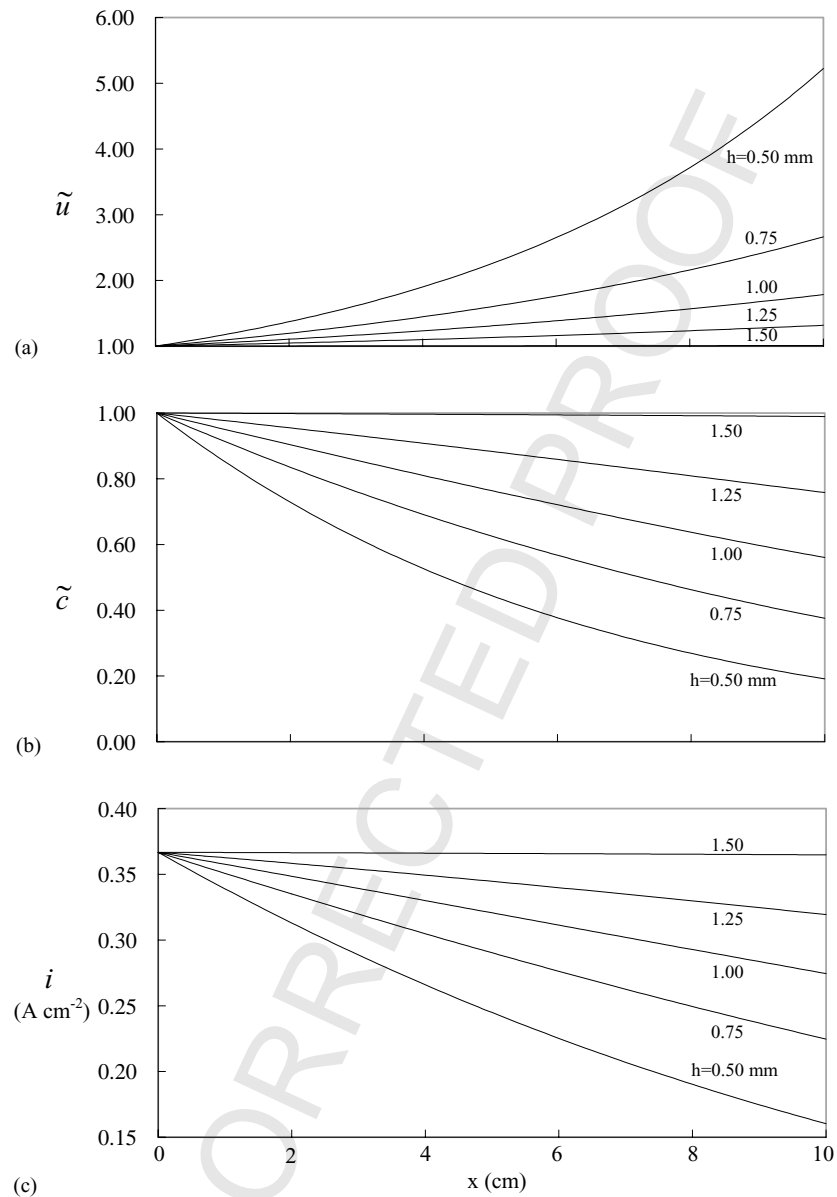


Fig. 6. Effects of channel height on along-the-channel variations of: (a) dimensionless velocity \tilde{u} ; (b) dimensionless concentration \tilde{c} ; (c) local current density.

349 a greater mass of the fuel per unit length, or a more suffi-
 350 cient supply of the fuel. Five different heights of channel are
 351 considered, viz., $h = 0.5, 0.75, 1.0, 1.25$ and 1.5 mm; the
 352 results are shown in Fig. 6(a)–(c). It is seen that a smaller
 353 height of channel leads to a larger increase in flow velocity
 354 and a larger decrease in fuel concentration along the chan-
 355 nel. Alternatively, small height of channel results in a larger
 356 decrease of local current density along the channel and thus
 357 a smaller power density (or a worse performance) for the
 358 fuel cell. Note that, since both the flow velocity and the fuel
 359 concentration have been normalized by the corresponding
 360 inlet conditions, a larger decrease of fact concentration in
 361 fact accounts for a smaller amount of fuel consumed along
 362 the channel. According to these results, the application can
 363 be made as follows. To have a fuel cell of higher fuel ef-
 364 ficiency, it is necessary to have a larger height of channel
 365 because the fuel can be consumed more efficiently. Corre-
 366 spondingly, to have a fuel cell of higher power density, it is

necessary to have height of channel so that a larger amount
 of fuel can be supplied.

4.5. Effect of porosity of gas-diffusion layer

The change in porosity of the gas-diffusion layer can be
 reflected in the present model by changing the parameter ξ
 at the bottom boundary. Physically, as mentioned above, a
 larger ξ means a larger porosity of the gas-diffusion layer.
 Five cases are considered, namely, $\xi = 0.1, 0.2, 0.3, 0.5$ and
 1.0. The results show that a larger ξ (or a larger porosity)
 results in a smaller increase in flow velocity (Fig. 7(a)) as
 well as a smaller decrease in fuel concentration (Fig. 7(b))
 because a larger portion of fuel is allowed to be sucked into
 the porous boundary at the bottom due to the larger porosity.
 Accordingly, a greater chemical reaction occurs in the
 gas-diffusion layer and leads to a uniformly high current den-
 sity along the channel (Fig. 7(c)). Accordingly, as discussed

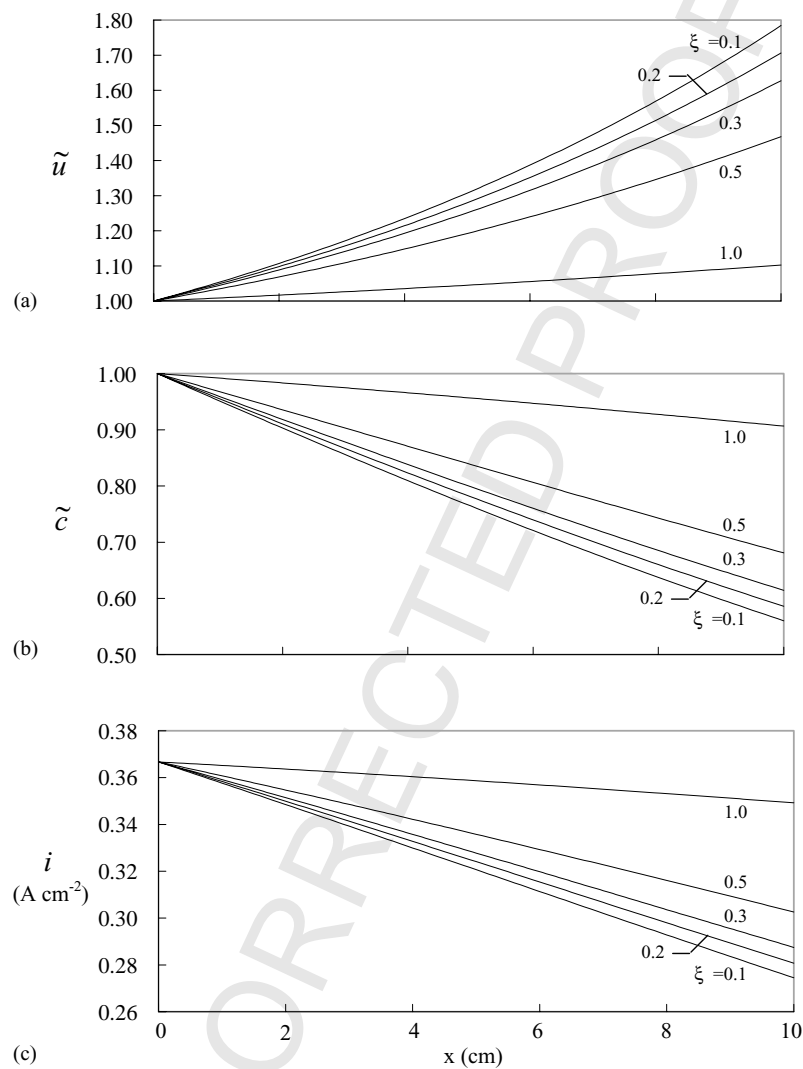


Fig. 7. Effects of porosity of gas-diffusion layer accounted for by parameter ξ on along-the-channel variations of: (a) dimensionless velocity \tilde{u} ; (b) dimensionless concentration \tilde{c} ; (c) local current density.

in above, a fuel cell with higher power density requires a larger porosity of the gas-diffusion layer to maintain a uniformly high current density along the channel. This conclusion is consistent with previous analyses of the optimization of the porosity of the gas-diffusion layer ([26], and references therein) which show that a higher porosity gives better performance of the fuel cell because in the gas-diffusion layer a larger space (or pores) is given to the water transportation so that the flooding can be prevented in high power density regimes. Thus, a larger porosity of the gas-diffusion layer is preferred for a fuel cell with a high power density.

5. Concluding remarks

A theoretical model for two-dimensional flow in fuel channels has been developed. This allows calculation of variations in fuel velocity, fuel concentration, and current density along the channel. The resultant ordinary equations and the initial conditions at the inlet of the channel consist of an initial value problem, which can be easily solved by a straightforward shooting scheme. The combination of the simplified equation model and the popular shooting scheme becomes a convenient, as well as an efficient, scheme for the design of fuel cell channels, such that several design and operation parameters can be determined for a fuel cell with either high power density or high fuel efficiency.

To have a fuel cell of high power density, results obtained in the present study suggest that it is necessary to: (i) increase the inlet velocity of fuel; (ii) increase the inlet pressure of fuel; (iii) decrease the height of fuel channel; and/or (iv) increase the porosity of the gas-diffusion layer. These four schemes also apply to fuel cell with longer fuel channels (or a larger size). Nevertheless, a high power density is always followed with a high fuel consumption rate, which results in a low fuel efficiency. In other words, to enhance the fuel efficiency of a cell or to apply a fuel cell with shorter fuel channels (or smaller size), it is necessary to apply a lower inlet velocity and/or a lower inlet pressure so that the fuel has a sufficiently long time to react with the catalyst in the gas-diffusion layer at the bottom. With the same reason, a channel with a larger height as well as a gas-diffusion layer with a smaller porosity will also help enhance the fuel efficiency (or shorten the channel length). Results show further that a catalyst of high activity is always a most desirable for fuel cell design because it gives a high power density while the accompanied efficiency loss is virtually negligible.

The above conclusions, nevertheless, are made only in qualitative senses; namely, they give only a trend for the design consideration. To obtain useful data for a quantitative design, experiments must be implemented to determine

some relevant parameters used in the simplified model. Particularly, the value of ξ cannot be determined without going through a series of experiments in which the porosity of the gas-diffusion layer is varied.

Acknowledgements

The authors are grateful for the financial support for this research through the following research grants of National Science Council of Taiwan: NSC 92-2623-7-002-006-ET and NSC 91-2218-E-211-001.

References

- [1] T.N. Veziroglu, *Int. J. Hydrogen Energy* 25 (2000) 1143–1150.
- [2] J. Larminie, A. Dicks, *Fuel Cell Systems Explained*, Wiley, UK, 2000.
- [3] P. Costamagna, S. Srinivasan, *J. Power Sources* 102 (2001) 242–252.
- [4] P. Costamagna, S. Srinivasan, *J. Power Sources* 102 (2001) 269.
- [5] A.S. Aricò, P. Cretì, V. Baglio, E. Modica, V. Antonucci, *J. Power Sources* 91 (2000) 202–209.
- [6] D.M. Bernardi, M.W. Verbrugge, *AIChE J.* 37 (1991) 1151–1163.
- [7] D.M. Bernardi, M.W. Verbrugge, *J. Electrochem. Soc.* 139 (1992) 2477–2491.
- [8] T.E. Springer, T.A. Zawodzinski, S. Gottesfeld, *J. Electrochem. Soc.* 138 (1991) 2334–2342.
- [9] T.F. Fuller, J. Newman, *J. Electrochem. Soc.* 140 (1993) 1218–1225.
- [10] T.V. Nguyen, R.E. White, *J. Electrochem. Soc.* 140 (1993) 2178–2186.
- [11] J.S. Yi, T.V. Nguyen, *J. Electrochem. Soc.* 145 (1998) 1149–1159.
- [12] A.A. Kornyshev, A.A. Kulikovskiy, *Electrochim. Acta* 46 (2001) 4389–4395.
- [13] H. Dohle, A.A. Kornyshev, A.A. Kulikovskiy, J. Mergel, D. Stolten, *J. Electrochem. Commun.* 3 (2001) 73–80.
- [14] A.A. Kulikovskiy, *J. Electrochem. Commun.* 3 (2001) 572–579.
- [15] P. Argyropoulos, K. Scott, W.M. Taama, *J. Chem. Eng.* 73 (1999) 217–227.
- [16] P. Argyropoulos, K. Scoff, W.M. Taama, *J. Chem. Eng.* 73 (1999) 229–245.
- [17] P. Argyropoulos, K. Scott, W.M. Taama, *J. Power Sources* 79 (1999) 169–183.
- [18] P. Argyropoulos, K. Scott, W.M. Taama, *J. Power Sources* 79 (1999) 184–198.
- [19] P. Argyropoulos, K. Scott, W.M. Taama, *J. Chem. Eng.* 78 (2000) 29–41.
- [20] P. Futerko, I.-M. Hsing, *Electrochim. Acta* 45 (2000) 1741–1751.
- [21] D. Thirumalai, R.E. White, *J. Electrochem. Soc.* 144 (1997) 1717–1722.
- [22] Z.H. Wang, C.Y. Wang, K.S. Chen, *J. Power Sources* 94 (2001) 40–50.
- [23] U.M. Sukkee, C.-Y. Wang, K.S. Chen, *J. Electrochem. Soc.* 147 (12) (2001) 4485–4493.
- [24] G.S. Beavers, D.D. Joseph, *J. Fluid Mech.* 30 (1967) 197–207.
- [25] H.E. Huppert, *J. Fluid Mech.* 121 (1982) 43–58.
- [26] Z. Qi, A. Kaufman, *J. Power Sources* 109 (2002) 38–46.